Analysis of Climb Trajectory Modeling for Separation Assurance Automation

David P. Thipphavong*
NASA Ames Research Center, Moffett Field, CA, 94035

Climb prediction uncertainty is a major source of error in trajectory-based automation for air traffic management. In this study, the performance of a trajectory-based automated separation assurance system is analyzed under different levels of uncertainty in laboratory simulations to investigate its robustness to climb uncertainty. Results indicate that this fully automated system can successfully detect and resolve 99% of conflicts in the high-altitude sectors of Fort Worth Center during 3-20 minutes prior to first loss of separation under near-zero uncertainty. Trajectory uncertainty was then incorporated into the simulation in the form of weight uncertainty. System performance remained unchanged for these scenarios when weight uncertainties ranged ± 10%. However, performance declined to 87% when this range was expanded to ± 20%.

Nomenclature

$a(t)_{error}$	=	along-track error (nmi)
D	=	drag (lb)
g	=	acceleration of gravity (ft/sec^2)
h	=	altitude (ft)
$h(t)_{error}$	=	altitude error (ft)
$h(t)_{pred}$	=	predicted altitude at time t (ft)
$h(t)_{track}$	=	radar track altitude at time t (ft)
L	=	lift (lb)
m	=	aircraft mass (lb)
T	=	engine thrust (lb)
V_g	=	ground speed (kt)
V_t	=	true airspeed (kt)
W_l	=	horizontal wind magnitude (kt)
x, y	=	east and north position (nmi)
$x(t)_{pred}$	=	predicted x-position at time t (nmi)
$x(t)_{track}$	=	radar track x-position at time t (nmi)
$y(t)_{pred}$	=	predicted y-position at time t (nmi)
$y(t)_{track}$	=	radar track y-position at time t (nmi)
γ_a, γ_i	=	air-relative and inertial flight-path angle (deg)
ϕ_a	=	aerodynamic bank angle deg (deg)
ψ_i	=	inertial heading (deg)
$\psi(t)_{pred}$	=	predicted course at time t (deg)
ψ_{rel}	=	relative wind angle, $\psi_i - \psi_w$ (deg)
ψ_w	=	wind direction (deg)

I. Introduction

Controller workload is a primary factor limiting airspace capacity, and air traffic demand is expected to increase substantially over the next 20 years [1]. Numerous concepts to increase airspace capacity through higher levels

* Aerospace Engineer, Automation Concepts Research Branch, David.P.Thipphavong@nasa.gov, AIAA Member.

of automation have been proposed in recent years [2-6]. Previous research on automated conflict resolution algorithms in fast-time simulations showed that more than 99% of conflicts could be resolved automatically for 1x, 2x, and 3x of today's air traffic demand [7,8]. However, these simulations were conducted without uncertainties. It is important to determine how well these algorithms perform in the presence of uncertainty, because prediction accuracy and robustness [9-13] is important for any trajectory-based automated separation assurance (SA) system. Recent research on trajectory-based SA automation found that late conflict detection due to climb uncertainty is the most common reason for automated conflict resolution failure [14].

This study differs from earlier research on how trajectory uncertainty affects the performance of SA automation systems because the uncertainty being incorporated into the simulations of this study was controlled. Uncertainty present in the simulations of [14] was mainly due to inherent differences between the aircraft models used by the flight simulator and the Trajectory Synthesizer (TS) module of the Center/TRACON Automation System (CTAS) that generated trajectory predictions. These include differences in aircraft weight, speed profiles, turn dynamics, waypoint capture logic, and thrust models. The current study evaluates SA automation performance in the presence of user-specified levels of uncertainty. However, as in [14], the analysis presented here focuses on strategic separation in the 3-20 minute time horizon for operations in Fort Worth Center at or above flight level 240.

Section II introduces the equations of motion used by the TS to generate trajectory predictions in this study, and discusses the effect that uncertainty can have on climb trajectory prediction accuracy. Section III presents the uncertainty characteristics of a high-fidelity trajectory modeler for two thousand "clean" (i.e., uninterrupted by level segments, descent segments, flightplan amendments, etc.) departures in the Dallas/Fort Worth area. Altitude and along-track errors were calculated for look-ahead times of up to 12 minutes. Section IV partitions these results by aircraft type to determine the contribution of aircraft performance modeling errors and environmental factors in climb trajectory uncertainty. Section V analyzes the sensitivity of climb predictions to weight variation with respect to current minimum separation criteria and the observed weight variation in current operations. Section VI describes the simulation methodology that was used to measure the effect of trajectory uncertainty on SA automation, presents a mechanism for incorporating controllable levels of uncertainty, and specifies the performance metric used. Section VII evaluates SA automation in a near-zero uncertainty environment. Section VIII analyzes the climb trajectory uncertainty characteristics of the simulations under different levels of weight uncertainty, and evaluates SA automation as a function of weight uncertainty. Section IX concludes the paper.

II. Equations of Motion

This section introduces the equations of motion used to generate the trajectory predictions in this study and develops some intuition about the potential effect of uncertainty on climb trajectory prediction accuracy. These equations of motion were presented in [15], and are reproduced below for convenience. Additional detail regarding the definitions of the angles and speeds used in these equations can be found in the "Equations of Motion" section of [15]. Information on the integration methods used to generate trajectories can be found in the subsequent sections of that paper.

$$\dot{V}_t = \frac{T - D}{m} - g\gamma_a - \frac{d(W_l \cos\psi_{rel})}{dt} \tag{1}$$

$$L = mg \tag{2}$$

$$\dot{h} = V_t \gamma_a = V_g \gamma_i \tag{3}$$

$$\dot{\psi}_i = \frac{L \sin\phi_a}{m V_g} \tag{4}$$

$$\dot{x} = V_g \sin\psi_i \tag{5}$$

$$\dot{y} = V_g \cos\psi_i \tag{6}$$

$$\dot{m} = 0 \tag{7}$$

From Equations 1 and 3, uncertainty in aircraft mass (m), thrust (T), drag (D), horizontal wind magnitude (W_l) and relative wind angle ($\psi_{rel} = \psi_i - \psi_w$) affects altitude trajectory prediction accuracy through the growth rate of true airspeed ($\dot{V}_t$). However, uncertainty in these parameters also affects along-track prediction errors because ground speed is equal to true airspeed plus a wind factor, and ground speed is an input into Equations 4-6. As such, the magnitude and distribution of both altitude and along-track errors are expected to change in the sensitivity analysis of trajectory predictions to weight variation presented in Section V. However, the first task is to determine how accurate nominal CTAS trajectory predictions are relative to actual flight paths.

III. Climb Prediction Uncertainty

This section analyzes the accuracy of a high-fidelity real-time trajectory prediction modeler for climbing departures in the Dallas/Fort Worth area. Trajectory predictions from the Trajectory Synthesizer (TS) module of the Center-TRACON Automation System (CTAS) are generated using enroute Center Host track and flightplan data (updated every 12 secs for all flights), hourly updates of atmospheric condition forecasts (e.g., wind, temperature, pressure) from the National Oceanic and Atmospheric Administration Rapid Update Cycle model, and a database of over 100 unique aircraft models. A more detailed description of these data sources can be found in Section II of [16]. Traffic data from 8:00 AM to 10:00 PM (local time) in the Fort Worth Air Route Traffic Control Center (ARTCC, or Center) for 14 days between mid-February and early March 2008 were used in this analysis. Although this section only focuses on climb prediction accuracy, the analysis can be applied to both level and descent trajectories as well as other trajectory prediction modelers.

The accuracy of TS predictions for climbing departures was analyzed by calculating altitude and along-track errors using the equations given in [13]. However, instead of segmenting flight paths as in [13], only departures that were not interrupted by level segments, descent segments, or flightplan amendments were included in this analysis. In this way, the effects of controller input and pilot intent on flight paths were removed as much as possible to allow for a more precise analysis of TS prediction accuracy. The 18000 ft altitude threshold was chosen so that flights could nominally have 4 minutes to achieve a steady climb speed following the 250 kt speed restriction at 10000 ft (assuming a nominal climb rate of 2000 ft/minute). The altitude and along-track errors at a given time t were calculated as follows:

$$h(t)_{error} = h(t)_{pred} - h(t)_{track} \tag{8}$$

$$a(t)_{error} = (x(t)_{pred} - x(t)_{track})\sin\psi(t)_{pred} + (y(t)_{pred} - y(t)_{track})\cos\psi(t)_{pred} \tag{9}$$

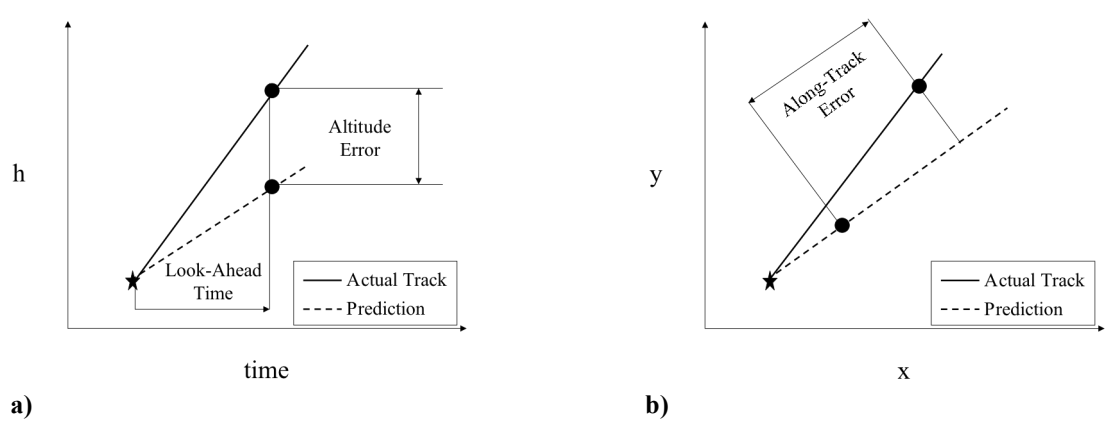

a) **b)**

Figure 1. Calculation of a) altitude and b) along-track errors for a "clean" climbing departure.

Histograms of the altitude and along-track trajectory prediction errors for "clean" climbing departures are shown in Figs 2 and 3 below for a look-ahead time of 5 minutes. Note that the standard deviation of the altitude errors exceeds twice the legal vertical separation limit of 1000 ft.

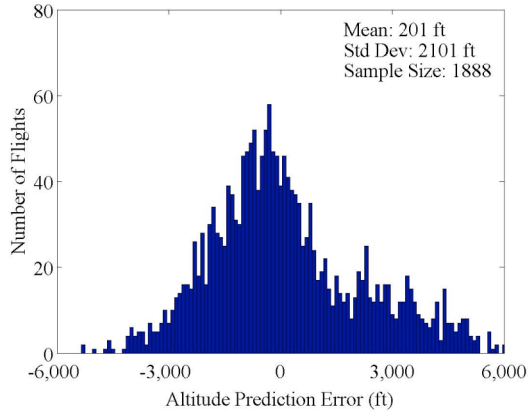

Figure 2: Climb trajectory altitude prediction errors for 5-minute look-ahead (Center Host radar track data)

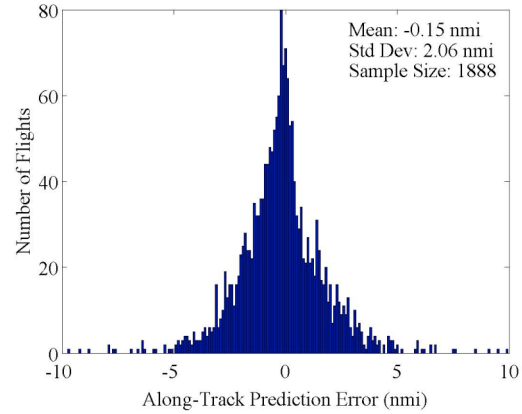

Figure 3. Climb trajectory along-track prediction errors for 5-minute look-ahead (Center Host radar track data).

Since trajectory prediction accuracy is a function of look-ahead time, it is important to compute and analyze the altitude and along-track errors for relevant look-ahead times. To that end, the altitude and along-track trajectory errors for "clean" climbing departures were calculated for look-ahead times of up to 12 minutes. The means and standard deviations of these altitude and along-track errors are presented in Figs 4 and 5, respectively. As expected the standard deviations grow as look-ahead time increases. It is interesting to note that the means are reasonably close to zero for all look-ahead times considered here. The next step is to probe deeper into the underlying causes of climb uncertainty by comparing the accuracy of CTAS trajectory predictions for different aircraft types.

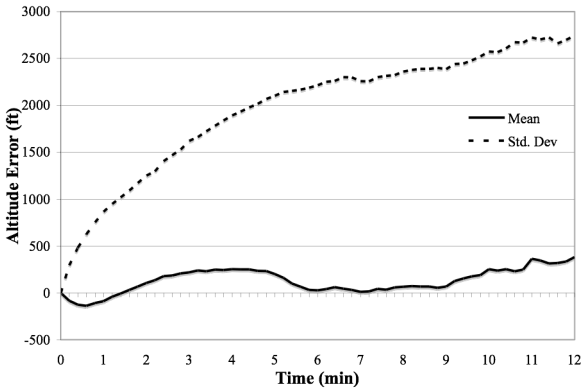

Figure 4. Climb trajectory altitude errors for look-ahead times of up to 12 minutes.

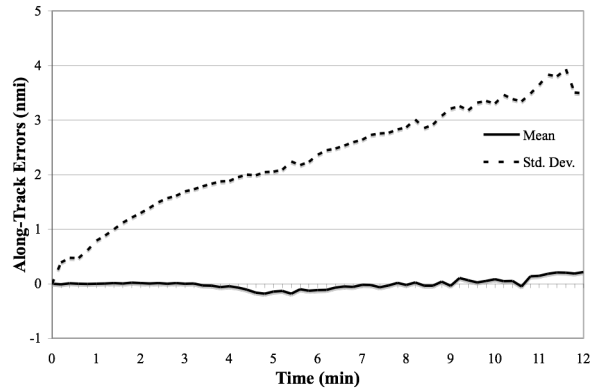

Figure 5. Climb trajectory along-track errors for look-ahead times of up to 12 minutes

IV. Variation of Climb Uncertainty Characteristics Among Aircraft Types

This section analyzes the variation in climb trajectory prediction accuracy among the 10 most common aircraft types in Fort Worth Center. These aircraft comprised about 85% of the available data. First, the altitude and along-track errors calculated for Section III were categorized by aircraft type. Then, the mean and standard deviation of these errors were calculated separately for each aircraft type; summary statistics of the 5-minute climb trajectory prediction errors were compiled into Table 1.

Aircraft Type	Mean of Altitude Errors (ft)	Standard Deviation of Altitude Errors (ft)	Mean of Along-Track Errors (nmi)	Standard Deviation of Along-Track Errors (nmi)	% of Sample Size (2119)
All Aircraft	201	2101	-0.15	2.06	100.0%
B733	462	1056	0.22	2.36	5.9
B735	-1317	1126	0.42	2.65	2.5
B737	-2125	1031	0.76	2.72	3.7
B738	-1658	1114	-0.30	2.13	4.4
B752	-963	1535	-0.18	2.88	4.0
CRJ7	-1330	1734	-0.24	1.50	5.5
E135	2722	1440	-0.04	1.81	6.7
E145	3191	1230	0.04	2.00	14.4
MD82	-568	1006	-0.43	1.75	26.6
MD83	-259	996	-0.30	1.99	11.0

Table 1. Climb trajectory errors for a 5-minute look-ahead by aircraft type.

First, consider the wide variation in the altitude trajectory prediction error characteristics among aircraft types in Table 1. For example, the altitude errors for MD83 aircraft have a mean of -259 ft and standard deviation of 996 ft. By comparison, the altitude errors for E145 aircraft have a greater mean of 3191 ft, and those for CRJ7 aircraft have a larger standard deviation of 1734 ft. This wide variation in vertical climb trajectory accuracy among aircraft types indicates that the performance models of some aircraft such as the MD82 and MD83 are more accurate than others like the E135 and E145. Since the MD8 aircraft performance model was analyzed and the climb prediction accuracy of the TS for this aircraft type was improved in previous research [12], this analysis suggests that adjusting the performance models of the other aircraft types in Table 1 in a similar manner can have a strong effect on the overall trajectory accuracy of the TS for climbing aircraft in the vertical dimension.

Next, consider the variation in the along-track error characteristics among aircraft types in Table 1. The along-track mean errors range from -0.43 nmi (MD82) to 0.76 nmi (B737), and the standard deviations range from 1.50 nmi (CRJ7) to 2.88 nmi (B752) for a 5-minute look-ahead time. Although trajectory prediction accuracy for climbing aircraft varies significantly in the vertical dimension among aircraft types, it is similar among aircraft types in terms of along-track error. This analysis suggests that environmental factors such as wind, which affects all climbing aircraft, are the primary causes of the along-track errors observed here.

V. Sensitivity of Climb Predictions to Weight Variation

This section measures the sensitivity of CTAS climb trajectory forecasts to weight uncertainty. Recall that late conflict detection due to climb trajectory prediction uncertainty was the largest factor affecting automated conflict resolution performance [14]. The first step was to compute a set of trajectory predictions for each climbing aircraft using takeoff weights between 60% and 100% (in intervals of 5 percentage points) of the maximum takeoff weight for that aircraft's type. Then, the altitude and along-track errors for each of these trajectories were calculated using Equations 8 and 9 (in Section III). Lastly, the means of these altitude errors were calculated for each weight input and look-ahead time, and graphed in Fig 6 below.

Recall from Section III that the altitude prediction errors had a mean and standard deviation of 201 ft and 2101 ft, respectively, for a 5-minute look-ahead. The weight input used to generate these nominal predictions was equal to 90% of each aircraft type's maximum takeoff weight. In Fig 6 below, a -10 % weight input change (to 80%) resulted in a +1469 ft mean altitude prediction error while a +10% weight input change (to 100%) led to a -902 ft mean altitude prediction error for the same 5-minute look-ahead (denoted by the asterisks in the figure). Note that a 10% difference between the actual and modeled weights shifts the mean of the errors by about 1200 ft for a 5-minute prediction time, which is near the lower bound of the strategic time frame (3-20 min) for SA automation. This mean shift exceeds the current vertical separation standard. This is significant, since takeoff weight variation of more than 10% within aircraft types is common in current operations [10]. For instance, MD8 aircraft takeoff weights had a standard deviation equal to 7.1% of their mean. If these takeoff weights had a Gaussian distribution, then approximately 16% of MD8 aircraft had takeoff weights that deviated more than 10% from the mean. MD8 aircraft accounted for nearly 40% of the flights in Table 1. The other 10 common commercial aircraft types analyzed in [10] had weight standard deviations ranging from 3.9% to 20.1% of their respective means.

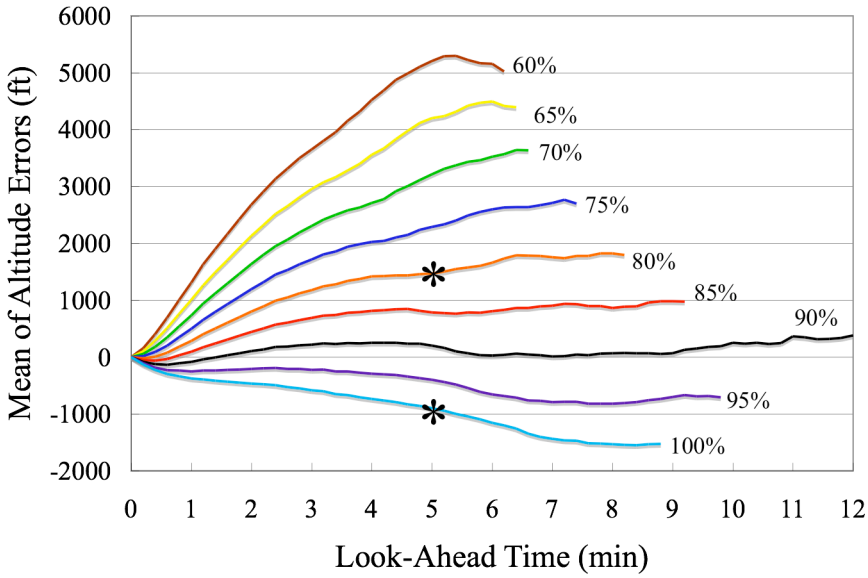

Figure 6. Effect of weight variation on altitude trajectory prediction errors.

For the along-track errors, the means and standard deviations are not sensitive to weight variation between 60% and 100%. For a 5-minute prediction, the means of the along-track errors range between -0.25 nmi and 0.20 nmi while the along-track standard deviations range from 1.99 nmi to 2.07 nmi. Further investigation revealed that the along-track error for individual aircraft changed as expected (based on the equations of motion presented in Section II), but the overall Gaussian distribution of the nominal along-track errors observed in Fig 3 (i.e., using a weight value equal to 90% of each aircraft type's maximum takeoff weight) did not change.

The sensitivity analysis of CTAS trajectory predictions to weight variation presented here can be extended to the other parameters discussed in Section II. However, these results provide preliminary insight into the potential effect that real-world aircraft parameter uncertainty can have on climb trajectory predictions and, consequently, the overall effectiveness of the SA automation. The next step in this analysis is to develop a simulation environment to evaluate SA automation performance under different levels of uncertainty.

VI. Simulation Methodology

This section describes the methodology used to incorporate trajectory uncertainty into SA simulations. Trajectory predictions were used for both flight simulation and conducting automated conflict detection and resolution, and were generated by the Trajectory Synthesizer module of CTAS using the same data discussed in Section III. Three 2-hour traffic scenarios over 5 different days (April 23-27, 2008) were used to evaluate SA automation performance in the near-zero uncertainty case. A subset of these scenarios with the heaviest traffic loads was used to evaluate the SA automation under different levels of uncertainty. The analysis conducted for this study focused on strategic separation for operations in Fort Worth Center high altitude airspace.

A. Generating Tracks in the CTAS Simulation Mode

The methodology is a variation of those used in [14] and [16] for previous CTAS simulation experiments. However, instead of using an independent aircraft track generator (e.g., PAS), the CTAS simulation mode used in this study generates track updates based on the trajectories generated by the TS module of CTAS. As such, with a few exceptions related to simulation heuristics and trajectory prediction heuristics (e.g., selection of downstream fix when the flight is near a fix), simulated flights fly the way the TS predicts. As such, the simulation is expected to have near-zero uncertainty. Since these same trajectory predictions are also used for automated conflict detection and resolution in the nominal CTAS simulation mode, the SA automation is expected to detect and resolve nearly all conflicts under near-zero uncertainty.

To begin, a recording of actual Host track and flightplan data for all flights in and around Fort Worth Center is passed into the CTAS automation. In the CTAS simulation mode, each aircraft flies according to its actual radar tracks until it achieves a user-specified initialization condition. For climbing aircraft, the radar track update where altitude passes 14000 ft is its simulation initialization point, or IP. This criterion was chosen so that these flights could nominally have 2 minutes to achieve a more steady climb speed following the 250 kt speed restriction at 10000 ft, and would nominally have 5 minutes of climbing flight for conflict detection (at a climb rate of 2000 ft/minute) until the lower boundary of high altitude airspace. Conflict resolution may also be performed during this time if a conflict is detected with more than 3 minutes until predicted first loss of separation, and that point is in a high-altitude sector. Active temporary altitudes for climbing flights are automatically removed by the simulation to keep them on steady climbs up to their flightplan altitude. For flights approaching the Fort Worth Center boundary from neighboring Centers, their fifth track update in the system is their IP. This allows the CTAS ground speed filter to stabilize and produce a more accurate airspeed for subsequent simulated tracks. Once a flight has initialized, all subsequent radar tracks and flightplan amendments recorded in the Host computers for that flight are ignored. Aircraft in the CTAS simulation mode automatically fly according to flightplan amendments generated by CTAS. Flights landing in or near Fort Worth Center automatically descend at their minimum-fuel top-of-descent point as computed by the TS.

B. Automated Conflict Detection and Resolution

Two types of simulations were run: (1) Open-loop simulations, in which CTAS simulated aircraft movement and performed conflict detection but did not attempt automated conflict resolution, and (2) Closed-loop simulations, in which CTAS generated trajectories and performed automatic conflict detection and resolution. The open-loop simulation provided a measure of the number of conflicts that the SA automation needed to detect and resolve. The closed-loop simulation gauged the ability of the system to detect and resolve conflicts. The conflict detection module was recently upgraded in CTAS [17] to update predicted traffic conflicts every 12 sec by comparing the most recent trajectory predictions available.

Automatic conflict resolution is attempted for all detected conflicts that meet the following criteria (the same criteria used in [14]):

- Predicted time to initial loss of separation is between 3 and 12 minutes, inclusive,
- Predicted separation of less than 8 nmi and 1000 ft when both aircraft are in level flight at first loss of separation,
- Predicted separation of less than 8 nmi and 1500 ft when one or both aircraft are climbing or descending at first loss of separation,
- Predicted conflict is not between two aircraft merging to a common arrival metering fix, and
- Predicted initial loss of separation is at or above FL240 and inside Fort Worth Center.

The expanded separation criteria of 8 nmi and 1500 ft for conflict pairs involving transitioning aircraft helps to account for the higher trajectory prediction uncertainty (compared to conflicts between two level flights). Conflict resolution for arrivals merging to a common meter fix has been explored [18,19], but it is beyond the scope of this study. Conflicts are detected out to a 20-minute time horizon, but conflict resolutions are not attempted until the predicted time to first loss of separation falls to 12 minutes or less.

The automatic conflict resolution algorithm being developed and tested at NASA Ames [20,21] was integrated into CTAS. Trial resolutions are modeled after the flight plan, altitude, and speed profile changes that controllers routinely issue to pilots in today's operations. Each conflict is first assigned to one of several categories that define the set of acceptable resolution maneuvers for the conflict pair and the preferred flight to be maneuvered. The TS generates a 4D trajectory for each trial resolution maneuver one at a time. If the resulting trajectory is conflict-free, the maneuver is sent to the aircraft, which then executes it. Otherwise, the algorithm automatically continues to generate a 4D trajectory for the next preferred maneuver and probe it for conflicts until a conflict-free resolution is found. Resolution maneuvers are chosen based on the following criteria (the same criteria used in [14]):

- Predicted separation of more than 10 nmi or 1000 ft when both aircraft are in level flight at first loss of separation,
- Predicted separation of more than 10 nmi or 2000 ft when one or both aircraft are climbing or descending at first loss of separation,

- Resolution trajectory is conflict-free for at least 20 minutes from the time the resolution amendment is entered,
- Predicted first loss of separation is more than 3 minutes in the future,
- Maximum turn angle of 45 deg for auxiliary waypoint route amendment resolution trajectories,
- Maximum range of 350 nmi to downstream capture fix for auxiliary waypoint resolutions, and
- Increments of 1000 ft for climb and descent maneuvers.

C. Incorporating Uncertainty into the CTAS Simulation Mode

Both open- and closed-loop simulations were conducted in the near-zero uncertainty CTAS simulation mode to establish a baseline performance level for the SA automation. However, since the main objective was to determine how uncertainty affects the performance of this system, a mechanism was needed to incorporate uncertainty into the simulation. The method developed was to select a parameter (e.g., weight), and have a random number generator assign each flight a perturbation amount for that parameter. Flights were simulated in CTAS with these perturbations applied. However, trajectories for the SA automation were generated without perturbations. Note that the versatility of this mechanism allows for uncertainty in parameters such as weight, wind, and speed profile to be incorporated into the simulation both separately and simultaneously.

D. Performance Metric

The metric used in this study to assess the performance of the SA automation in CTAS is given below:

$$\text{SA Automation Performance} = 1 - \frac{\text{closed loop losses of separation}}{\text{open loop losses of separation}} \tag{10}$$

It is the same metric used in [14], to allow for direct comparison. As such, both open- and closed-loop simulations were conducted and analyzed for each traffic scenario. As mentioned earlier, the open-loop simulation results provided a baseline for the number of conflicts that the SA automation had to detect and resolve, and the closed-loop simulation results measured how well the SA automation maintain safe separation. The values for the performance metric in the near-zero uncertainty simulations serve as a baseline for simulations with different levels of uncertainty.

For every closed-loop simulation run, each loss of separation was examined to determine if it was due to 1) a trajectory-based automation error (trajectory modeling, conflict detection, or conflict resolution), or 2) a simulation error. For example, if climb uncertainty caused a conflict to not be detected until loss of separation occurs, then it was classified as a trajectory-based automation error. However, occasionally, flights were initialized late, violated current legal separation standards while flying into a high-altitude sector, or did not execute a resolution flightplan amendment. If these cases resulted in a loss of separation, then they were considered simulation errors. For this analysis, the number of closed-loop losses used in the performance metric was the only the sum of losses due to trajectory-based automation errors.

VII. Performance in the Presence of Near-Zero Uncertainty

Histograms of the altitude and along-track trajectory prediction errors for simulated climbing departures in the open-loop CTAS simulation mode are shown in Figs 7 and 8 for a look-ahead time of 5 minutes. The mean of the altitude errors is 311 ft, and the standard deviation is 109 ft. Vertical uncertainty for climbing aircraft in the nominal CTAS simulation mode is satisfactorily close to zero with an RMS value that is on the order of 20% of the vertical separation criteria used during conflict detection. Research is ongoing to calibrate these errors by addressing the underlying simulation and prediction heuristics. In addition, the mean of the along-track errors is 0.03 nmi, and the standard deviation is 0.50 nmi, which are also reasonably close to zero. None of these flights have trajectory uncertainty exceeding the current legal separation standard of 5 nmi laterally and 1000 ft vertically.

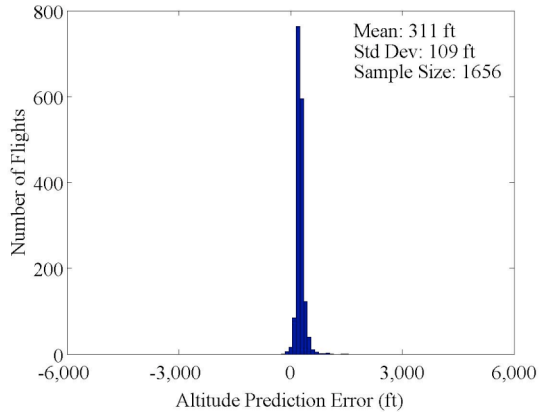

Figure 7. Climb trajectory altitude prediction errors for 5-minute look-ahead (CTAS simulation mode).

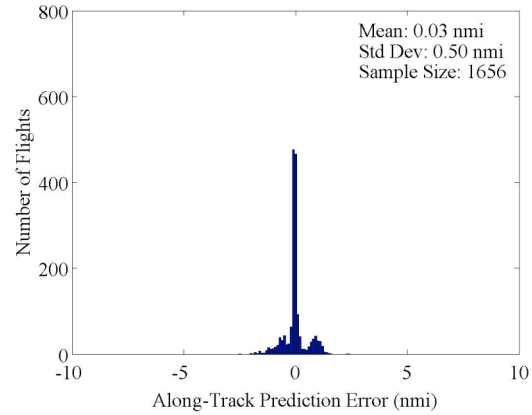

Figure 8. Climb trajectory along-track prediction errors for 5-minute look-ahead (CTAS simulation mode).

Closed-loop simulations were also conducted to evaluate SA automation performance in the CTAS simulation mode. Results are summarized in Table 2. Although overall SA automation performance is 99%, there is a noticeable difference in the performance metric between the 2-4 PM time period and the 4-6 PM and 6-8 PM time periods. The performance for the 4-6 PM and 6-8 PM time periods average to 100% over the 5 scenario days while the cumulative performance for the 2-4 PM time period is 97%. This is because the nominal CTAS simulation mode is not free of uncertainty (Figs 7-8). In fact, further analysis of the 5 flight pairs that lost separation found 1 case where a conflict-free resolution was not found, and 1 case where no trajectory was generated for conflict probing. Of the three remaining cases, two were due to erroneous conflict filtering (i.e. no resolution attempted), and one was due to an anomalous descent clearance by the simulation. If these three cases were excluded, then cumulative SA performance for the 2-4 PM period would be 99%, and overall SA automation performance would be 99.5%.

	Time Period (local time)			
Scenario Date	**2-4 PM**	**4-6 PM**	**6- 8 PM**	**SA Performance Metric (Day)**
4/23/2008	100%	100%	100%	**100%**
4/24/2008	92%	100%	100%	**97%**
4/25/2008	97%	100%	100%	**99%**
4/26/2008	100%	100%	100%	**100%**
4/27/2008	96%	100%	100%	**99%**
SA Performance Metric (Period)	**97%**	**100%**	**100%**	

Table 2. Automated SA Performance Under Near-Zero Uncertainty.

VIII. Performance in the Presence of Weight Uncertainty

This section presents preliminary analysis on the effect of trajectory prediction uncertainty on automated conflict detection and resolution performance. The experiments conducted for this section are identical to those conducted for Section VII except that uncertainty in aircraft weight was incorporated into the near-zero simulation. Weight uncertainty was the first type of uncertainty chosen because it has a significant effect on climb trajectory modeling, and prior research on takeoff weights for common aircraft types observed that weight variation of more than 10% is common in current operations [10]. Three cases were considered: (1) weight uncertainty uniformly distributed between -10% and +10% (of each aircraft's maximum takeoff weight in the CTAS aircraft database), (2) weight uncertainty uniformly distributed between -15% and +15%, and (3) weight uncertainty uniformly distributed between -20% and +20%. The 4-6 PM scenarios from Section VII were chosen for the experiments in this section because traffic in Fort Worth Center was busiest during that time period on those days, and the system was able to achieve an average of 100% performance in the near-zero uncertainty case for this subset of traffic scenarios.

A. Climb Uncertainty as a Function of Weight Uncertainty

Histograms of altitude and along-track trajectory prediction errors for the open-loop CTAS simulation mode with weight uncertainties that were uniformly distributed between -10% and +10% (Figs 9-10), between -15% and +15% (Figs 11-12), and between -20% and +20% (Figs 13-14) are shown below for a look-ahead time of 5 minutes. The altitude and along-track errors have means close to zero, and the along-track errors have standard deviation of about 0.5 nmi in all 3 cases, However, the standard deviation of the altitude errors increases from 791 ft to 1091 ft to 1485 ft for the ± 10%, ± 15%, and ± 20% simulations, respectively. As expected, the range of trajectory altitude errors for climbing departures increases as the range of weight uncertainties increases. Although the uncertainty characteristics are different than those for current operations (see Section III), testing the SA automation under these different conditions provides useful insight into its robustness.

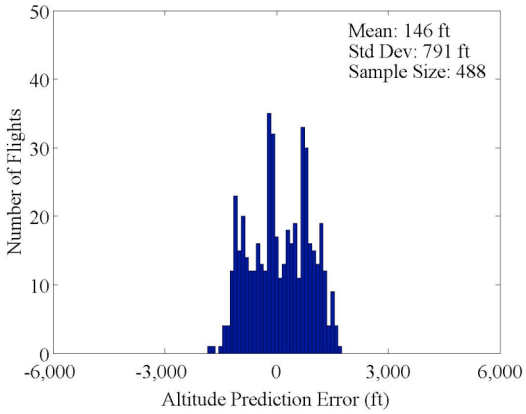

Figure 9. Climb trajectory altitude prediction errors for 5-minute look-ahead (± 10% weight uncertainty).

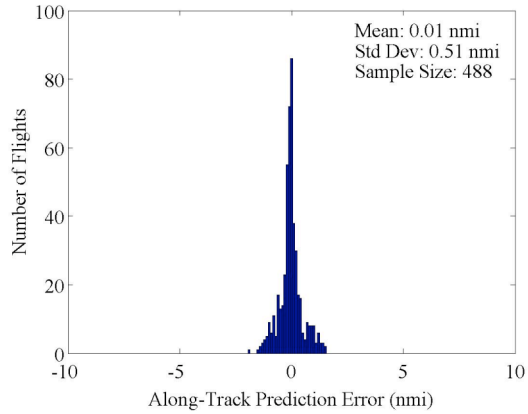

Figure 10. Climb trajectory along-track prediction errors for 5-minute look-ahead (± 10% weight uncertainty).

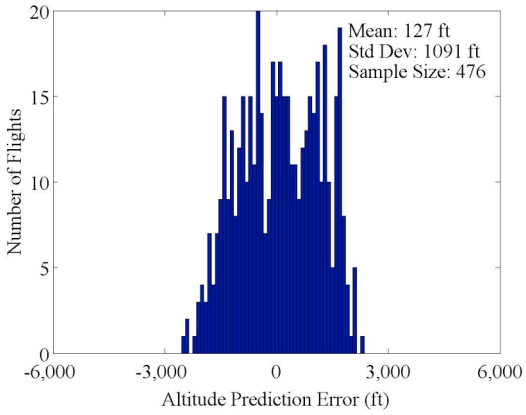

Figure 11. Climb trajectory altitude prediction errors for 5-minute look-ahead (± 15% weight uncertainty).

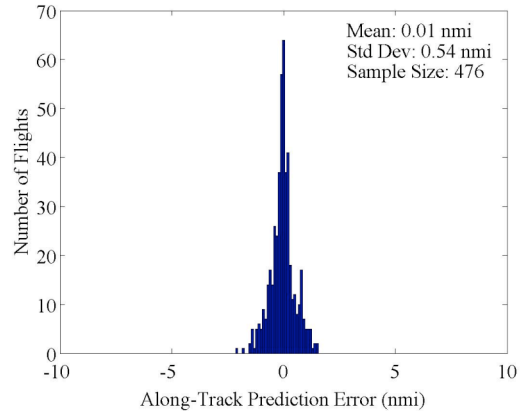

Figure 12. Climb trajectory along-track prediction errors for 5-minute look-ahead (± 15% weight uncertainty).

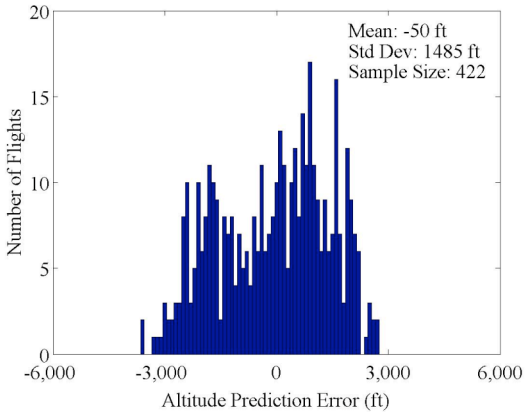

Figure 13. Climb trajectory altitude prediction errors for 5-minute look-ahead (± 20% weight uncertainty).

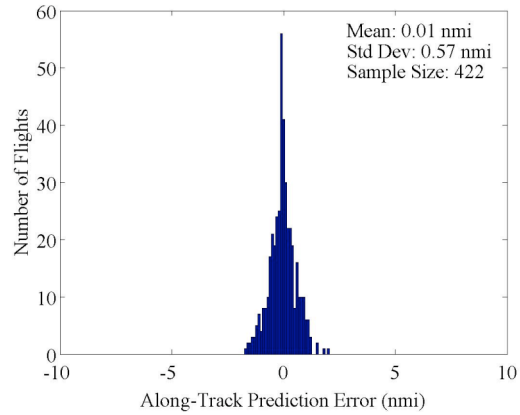

Figure 14. Climb trajectory along-track prediction errors for 5-minute look-ahead (± 20% weight uncertainty).

B. Performance Under Weight Uncertainty

Closed-loop simulations were also conducted to determine how well the SA automation performed under different levels of uncertainty, and the results are summarized in Table 3. It should be emphasized that these results may be dependent on the conflict detection and resolution criteria used (the same as in [14]). Recall that average SA performance for the set of scenarios used in this section was 100% (see the 4-6 PM column of Table 2) in the near-zero uncertainty case. SA automation performance remained steady at 100% when weight uncertainty in the simulation was uniformly distributed between -10% and +10%. These results may not seem to be in agreement with the sensitivity analysis of Section V, which showed that a 10% difference between actual and modeled aircraft weights increased average climb uncertainty by more than the current legal separation standard for a 5-minute prediction time. However, whether flights with large weight uncertainties maintain safe separation depends on how they interact with other flights. Additional simulations need to be conducted to ensure statistical significance for the results observed here, because the SA automation may not have been exposed to the full breadth and variety of conflict situations.

Three losses of separation were observed in the ± 15% case, resulting in a slight decline in system performance to 98%. A steep drop in SA automation performance to 87% can be seen when the range of weight uncertainties was increased to ± 20%. This is significant, because it is expected that any future automated SA capability will be required to detect and resolve well over 95% of conflicts on a strategic time horizon of 3-20 minutes prior to first loss of separation [14].

A detailed description of the 19 closed-loop losses of separation in the ± 20% simulations can be found in the Appendix. Fifteen of these cases were due to climb uncertainty, of which 9 involved late detection (less than 3 minutes prior to first loss) and 3 involved no detection. This implies that future research is necessary to enhance the robustness of the conflict detection module to climb uncertainty. Adding functionality to probe multiple climb trajectories ranging from low performance to high performance climbs [14] and expanding the conflict detection criteria are two possibilities. Although these approaches may reduce the number of late or missed detections, they could also increase delay due to unnecessary resolution maneuvers and the number of false alerts. This will be explored in future research to refine the results presented here.

	Range of Weight Uncertainties in the Simulation		
Scenario Date and Time	**± 10%**	**± 15%**	**± 20%**
4/23/2008, 4-6 PM	100%	97%	79%
4/24/2008, 4-6 PM	100%	100%	91%
4/25/2008, 4-6 PM	100%	97%	94%
4/26/2008, 4-6 PM	100%	100%	77%
4/27/2008, 4-6 PM	100%	96%	82%
SA Performance Metric (Overall)	**100%**	**98%**	**87%**

Table 3. Automated SA Performance Under Different Levels of Weight Uncertainty.

One additional caveat of the results presented in this section is that the distribution of the trajectory prediction errors in the weight uncertainty simulations was roughly uniform, which does not match the Gaussian distribution of errors observed for current operations in Section III. Fewer losses of separation may occur if a Gaussian distribution was used to generate weight uncertainties instead of a uniform distribution, because this would result in fewer flights with large weight errors. On the other hand, the magnitude of the climb trajectory prediction errors observed in the weight uncertainty simulations (Figs 9-14) is smaller than what was observed in practice (Figs 2-3). More losses of separation may occur if the simulation climb trajectory errors were increased to match those of current operations. Research is ongoing to incorporate trajectory uncertainty into the simulation using multiple sources of uncertainty (e.g., weight, wind, and speed profile) simultaneously to replicate both the distribution and the magnitude of the uncertainties observed in actual operations. The SA automation will be tested using this higher-fidelity simulation environment to refine the results presented here.

IX. Conclusions

The climb uncertainty characteristics of a high-fidelity trajectory modeler were analyzed by processing Center Host radar track and flightplan data for two thousand departures in the Dallas/Fort Worth area. Categorization of the altitude errors by aircraft type revealed that altitude prediction error characteristics varied greatly among aircraft types. The altitude errors of aircraft types whose performance models were analyzed and improved in previous research were smaller than the altitude errors of aircraft types that were not, which suggests that aircraft model improvements can have a strong impact on overall climb trajectory prediction accuracy.

A method was developed to measure the sensitivity of climb trajectory predictions to aircraft takeoff weight uncertainty. Results indicated that a 10% difference between the actual and modeled aircraft weights increased the magnitude of the altitude errors by about 1200 ft on average for a 5-minute look-ahead time. This is more than the current legal separation standard. This is significant, since prior research on takeoff weights for common aircraft types observed that weight variation of more than 10% is common in current operations.

In addition, the performance of a fully automated SA system was analyzed under different levels of uncertainty. Results indicated that this system could successfully resolve 99% of conflicts in the high-altitude sectors of Fort Worth Center given current traffic levels and near-zero uncertainty. Trajectory uncertainty was then incorporated into the simulation in the form of weight uncertainty for a subset of traffic scenarios where system performance averaged 100% under near-zero uncertainty. System performance remained at 100% when weight uncertainties ranged between -10% and +10%. A slight decline in SA automation performance to 98% was observed in the ± 15% case, and a steep drop to 87% was observed when the range of weight uncertainties was expanded to ± 20%. This finding is significant, because it is expected that any future automated SA capability will be required to detect and resolve well over 95% of conflicts on a strategic time horizon of 3-20 minutes prior to first loss of separation.

Appendix

Tables A1-A5 summarize the cases in which separation was lost in the ± 20% weight uncertainty simulations in Section VIII. The tables contain information about the aircraft type for both aircraft, the flight phase at predicted first loss of separation (climbing, level, or descending) for both aircraft, the lateral and vertical distance between aircraft at minimum separation, the conflict detection parameters (time to first loss in minutes, minimum predicted horizontal separation in nmi, and minimum predicted vertical separation in ft), the cause of the loss of separation based on post-simulation analysis, and whether the loss of separation was due to a trajectory-based automation error (T) or to a simulation error (S). A detailed description of simulation errors can be found in Section VI.

	AC1 (type)	AC2 (type)	Phase of Flight	Miss Distance (nmi, ft)	Conflict Detection (minutes, nmi, ft)	Cause of Loss of Separation	
1	E45X	SBR1	L/C	4.04, 455	3.4, 3.5, 883	no amendment, climb uncertainty	T
2	C56X	E145	C/C	3.31, 624	1.6, 2.2 1383	late detection, climb uncertainty	T
3	MD88	MD10	C/L	3.46, 243	1.8, 4.0, 971	late detection, climb uncertainty	T
4	B733	E45X	C/D	4.32, 386	4.7, 4.0, 1249	AC1 trajectory failure	T
5	MD82	MD82	C/L	4.60, 119	1.7, 2.4, 827	late detection, climb uncertainty	T
6	MD82	MD83	C/L	3.37, 275	2.0, 1.7, 827	late detection, climb uncertainty	T

Table A1. April 23, 2008 ± 20% closed-loop simulation.

	AC1 (type)	AC2 (type)	Phase of Flight	Miss Distance (nmi, ft)	Conflict Detection (minutes, nmi, ft)	Cause of Loss of Separation	
1	CRJ1	BE9L	C/L	2.57, 682	1.8, 1.7, 538	aircraft initialized with less than 3 minutes to go	S
2	FA20	A319	C/L	3.70, 8	2.3, 6.4, 946	late detection, climb uncertainty	T
3	WW24	DC87	C/L	2.66, 320	3.3, 6.5, 1402	late detection, climb uncertainty	T
4	DC10	B733	L/C	3.66, 668	2.3, 6.4, 902	late detection, climb uncertainty	T
5	CL30	B738	C/L	3.17, 573	no detection	no detection, climb uncertainty	T

Table A2. April 24, 2008 ± 20% closed-loop simulation.

	AC1 (type)	AC2 (type)	Phase of Flight	Miss Distance (nmi, ft)	Conflict Detection (minutes, nmi, ft)	Cause of Loss of Separation	
1	E135	B733	C/L	4.72, 646	no detection	no detection, climb uncertainty	T
2	E145	CRJ7	L/D	3.99, 355	8.3, 4.3, 794	resolution issued, conflict not resolved, descent uncertainty	T

Table A3. April 25, 2008 ± 20% closed-loop simulation.

	AC1 (type)	AC2 (type)	Phase of Flight	Miss Distance (nmi, ft)	Conflict Detection (minutes, nmi, ft)	Cause of Loss of Separation	
1	A306	MD82	L/C	4.98, 328	1.4, 6.4, 932	late detection, climb uncertainty	T
2	E145	A320	C/L	3.16, 695	4.9, 2.9, 868	resolution issued, conflict not resolved, climb uncertainty	T
3	MD83	DC10	C/L	3.77, 530	1.4, 2.3, 744	late detection, climb uncertainty	T

Table A4. April 26, 2008 ± 20% closed-loop simulation.

	AC1 (type)	AC2 (type)	Phase of Flight	Miss Distance (nmi, ft)	Conflict Detection (minutes, nmi, ft)	Cause of Loss of Separation	
1	LJ60	MD82	D/D	1.74, 915	4.6, 1.1, 949	no amendment, descent uncertainty	T
2	E135	B733	L/L	0.31, 736	19.5, 5.6, 0	AC1 trajectory failure	T
3	DC10	E145	L/C	4.04, 516	6.8, 7.1, 712	resolution issued, conflict not resolved, climb uncertainty	T
4	DC10	B733	L/C	4.37, 666	no detection	no detection, climb uncertainty	T

Table A5. April 27, 2008 ± 20% closed-loop simulation.

Acknowledgments

The author would like to thank David McNally, Chester Gong, Jeffery Schroeder, Russell Paielli, and Tamika Rentas for their insightful comments and suggestions, and John Robinson, Joe Walton, Don Shawver, Jinn-Hwei Cheng, Thien Vu, and Dave Darling for their support and development of CTAS software, without which this study would not have been possible.

References

[1]Joint Planning and Development Office, "Next Generation Air Transportation System Integrated Plan," Dec. 12, 2004.

[2]Erzberger, H., "Transforming the NAS: The Next Generation Air Traffic Control System," 24th International Congress of the Aeronautical Sciences, Aug. 29 – Sept. 3, 2004.

[3]Wing, D.J., Ballin, M.G., Krishnamurthy, K., "Pilot in Command: A Feasibility Assessment of Autonomous Flight Management Operations," 24th International Congress of the Aeronautical Sciences, Aug. 29 – Sept. 3, 2004.

[4]Barmore, B., Abbott, T., Krishnamurthy, K., "Airborne-Managed Spacing in Multiple Arrival Streams," 24th International Congress of the Aeronautical Sciences, Aug. 29 – Sept. 3, 2004.

[5]Battiste, V., Johnson, W.W., Holland, S., "Enabling Strategic Flight Deck Route Re-Planning Within A Modified ATC Environment: The Display of 4-D Intent Information on a CSD," Proceedings of the 2000 SAE World Aviation Congress and Exposition, Oct. 10-12, 2000.

[6]Prevot, T., Lee, P., Smith, N., Palmer, E., "ATC Technologies for Controller-Managed and Autonomous Flight Operations," AIAA Guidance, Navigation, and Control Conference, Aug. 15-18, 2005.

[7]Erzberger, H., "Automated Conflict Resolution for Air Traffic Control," 25th International Congress of the Aeronautical Sciences, Sept. 3-8, 2006.

[8]Farley, T., Erzberger, H., "Fast-Time Simulation Evaluation of a Conflict Resolution Algorithm under High Air Traffic Demand," 7th USA/Europe ATM 2007 R&D Seminar, July 2-5, 2007.

[9]Jackson, M.R., Zhao, Y.J., Slattery, R.A., "Sensitivity of Trajectory Prediction in Air Traffic Management," *Journal of Guidance, Control and Dynamics*, Vol. 22, No. 2, Mar.-Apr. 1999.

[10]Coppenbarger, R.A., "Climb Trajectory Prediction Enhancement Using Airline Flight-Planning Information," AIAA Guidance, Navigation, and Control Conference, Aug. 1999.

[11]Schwartz, B.E., Benjamin, S.G., Green, S.M., Jardin, M.R., "Accuracy of RUC-1 and RUC-2 Wind and Aircraft Trajectory forecasts by Comparison with ACARS Observations," *Weather Forecasting*, Vol. 15, 2000, pp. 313-326.

[12]Chan, W., Bach, R., Walton, J., "Improving and Validating CTAS Performance Models," AIAA Guidance, Navigation, and Control Conference and Exhibit, Aug. 14-17, 2000.

[13]Gong, C., McNally, D., "A Methodology for Automated Trajectory Prediction Analysis," AIAA Guidance, Navigation, and Control Conference and Exhibit, Aug. 16-19, 2004.

[14]McNally, D. and Thipphavong, D., "Analysis of Separation Assurance Automation in the Presence of Trajectory Uncertainty," 26th International Congress of the Aeronautical Sciences, Sept. 14-19, 2008.

[15]Slattery, R., Zhao, Y., "Trajectory Synthesis for Air Traffic Automation," *Journal of Guidance, Control and Dynamics*, Vol. 20, No. 2, Mar.-Apr. 1997.

[16]McNally, D., Gong, C., "Concept and Laboratory Analysis of Trajectory-Based Automation for Separation Assurance," AIAA Guidance, Navigation, and Control Conference, Aug. 21-24, 2006.

[17]Murphy, J, Robinson, J. (2007), "Design of a Research Platform for En Route Conflict Detection and Resolution," AIAA Aviation Technology Integration and Operations Conference, Sept. 18-20, 2007.

[18]Farley, T., Kupfer, M., Erzberger, H. (2007), "Automated Conflict Resolution: A Simulation Evaluation Under High Demand Including Merging Arrivals," AIAA Aviation Technology Integration and Operations Conference, Sept. 18-20, 2007.

[19]Kupfer, M., Farley, T., Chu, Y., Erzberger, H. (2008), "Automated Conflict Resolution – A Simulation-Based Sensitivity Study of Airspace and Demand," 26th International Congress of the Aeronautical Sciences, Sept. 14-19, 2008

[20]Erzberger, H. (2006), "Automated Conflict Resolution for Air Traffic Control," 25th International Congress of the Aeronautical Sciences (ICAS), Sept. 3-7, 2006.

[21]Prevot, T., Homola, J., Mercer, J. (2008), "Human in the Loop Evaluation of Ground-Based Automated Separation Assurance for NextGen," AIAA Aviation Technology Integration and Operations Conference, Sept. 14-19, 2008.